

SUMMARY, DIS 97¹

George Sterman

*Institute for Theoretical Physics
State University of New York at Stony Brook
Stony Brook, NY 11794-3840, USA*

Abstract

Some of the experimental and theoretical results discussed at the Fifth International Workshop on Deep Inelastic Scattering and QCD are reviewed.

1 Introduction

Each “DIS” workshop in this series has reflected exciting developments from the foregoing year in both theory and experiment. The Organizing Committee and Argonne National Laboratory have made possible another such meeting, distinguished by reports of progress in many directions, reflecting a vibrant and expanding field. DIS '97 was favored as well by strong participation from the hadron and e^+e^- collider communities. The timing for this participation could not have been better, given the fruitful interplay between these complementary arenas in the investigation of the strong interactions. We shall see examples repeatedly in what follows.

Let me begin with a summary of the Summary – a set of impressions of the past year for deeply inelastic scattering (DIS), as represented at this workshop. 1996-97 saw the culmination of a set of classic experiments, including final or near-final analyses from NMC [1], CCFR [2], SMC [3] and E154 [4]. Each has illuminated hadron structure [5] in a memorable fashion. From HERA [6, 7], we heard of increased coverage in the kinematic range in x and Q^2 , including reports on an excess of “large- x and Q^2 ” events [8, 9], which has drawn the attention of the press. The newly-rich study of DIS jet cross sections also affords a wealth of predictions that can be cross-checked in hadron-hadron collisions [10]. At the same time, a “coming-of-age” of diffraction and photoproduction [11] is making possible for the first time truly quantitative studies of these processes, at the boundary of perturbative and nonperturbative dynamics [12]. Finally, early results from HERMES are appearing in the fast-developing program of spin physics in DIS and elsewhere [13].

Theoretical developments [5, 12] reported at the conference were characterized by the requirements of “precision QCD”, a concept almost unimaginable fifteen, or even five, years ago. There is an across-the-board drive toward the calculation of

¹Presented at the Fifth International Workshop on Deep Inelastic Scattering and QCD, Chicago, IL, April 14-18, 1997.

higher-order corrections in perturbation theory, as well as toward the perturbative-nonperturbative interface, through resummed perturbation theory and related methods. The growing awareness of, and capability for, spin studies has reopened this field to perturbative QCD. Under the stimulus of new results, and projected experiments, theorists are reviving old ideas, inventing new directions, and, in general, struggling to keep up!

In the remainder of this summary, I can give only selected illustrations of these trends. It will hardly be possible to do justice even to the few topics I have space to discuss. More information may, of course, be found from the plenary talks at this conference, and from parallel sessions, and almost all the references will be to these.

That understood, I shall begin with a few observations on the excess of events at high Q^2 and x reported by H1 and ZEUS, which lead into an update on perturbative QCD in DIS and beyond [14, 15]. I will then turn to a review of generalizations of the factorization formalism that underlies perturbative QCD [16], from unpolarized to polarized scattering [17] and to diffraction [18]. I'll also say a few words about openings to nonperturbative QCD. Finally, I will conclude with some thoughts on where we are now, and where the field is going.

2 Structure Functions and the Excess at High Q^2

The DIS cross sections σ^\pm for $e^\pm - p$ scattering is conventionally presented in terms of the structure functions $F_2(x, Q^2)$, $F_3(x, Q^2)$ and $F_L(x, Q^2)$,

$$\frac{d\sigma^\pm}{dx dy} = \frac{2\pi\alpha^2 s}{Q^4} \left[\left(1 + (1-y)^2\right) F_2(x, Q^2) - y^2 F_L(x, Q^2) \mp \left(1 - (1-y)^2\right) F_3(x, Q^2) \right], \quad (1)$$

where as usual $x = Q^2/2p \cdot q$ is the scaling variable with $q^2 = -Q^2$, and $y = Q^2/xs$ is the fractional leptonic energy loss in the proton rest frame. Surely the most widely-recognized result from HERA this year is the excess of events found at high Q^2 and x (equivalently, high y and x), compared to the “standard model”, based on NLO QCD in DIS, as seen by ZEUS [19] and H1 [20]. Because the speculation engendered by these reports goes far beyond the QCD that goes into them, I will discuss their possible interpretation separately in this section, and only then return to QCD, and the standard model with which they have been compared.

It's an unexpected pleasure to comment on the large- Q^2 excess, although it is hardly possible to review the theoretical studies that have sprouted like so many flowers after a spring rain [12]. Surely it is, “about time”, for a new phenomenon, as it was so aptly observed. We shall have to wait and see, however, whether the time has truly come.

The events themselves are beautiful examples of the capabilities of the HERA detectors (Fig. 1), and of the imprint on hadronic final states of momentum transfers at short distances. The excess of events over the presently-available “standard model” is shown in terms of Q^2 in Fig. 2.

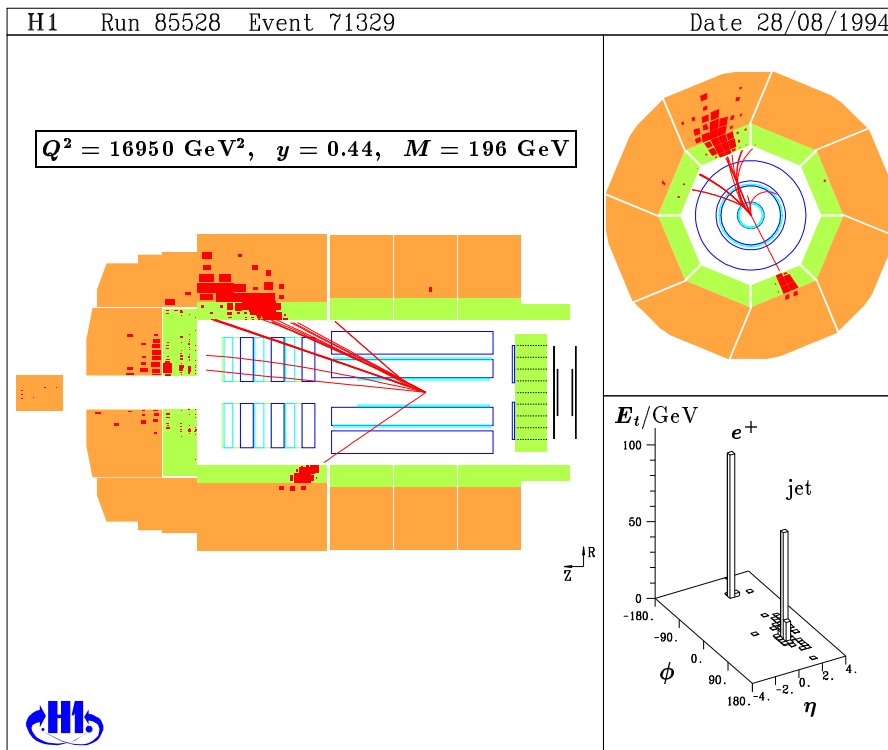
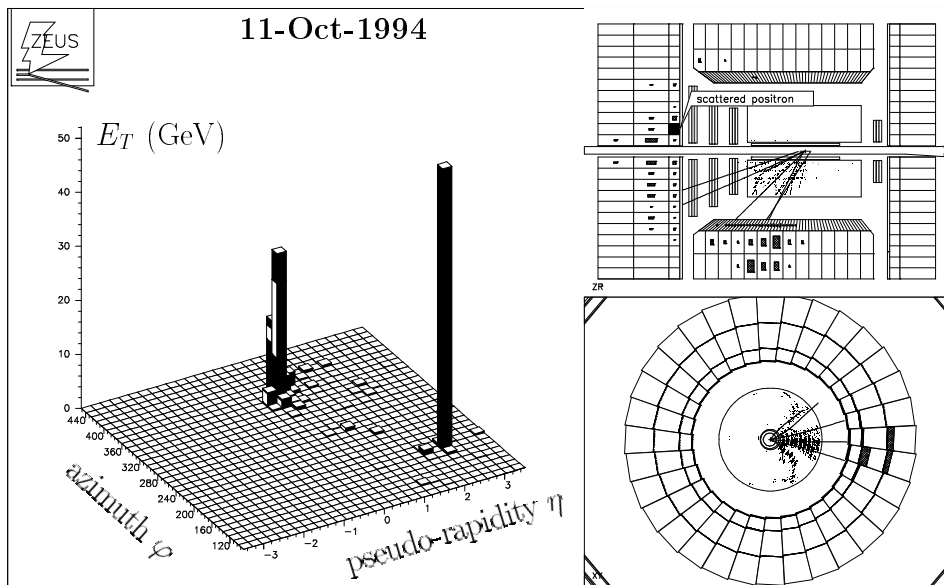


Figure 1: Neutral current events in the highest- Q^2 sample, as presented by ZEUS [19] (top) and H1 [20] (bottom).

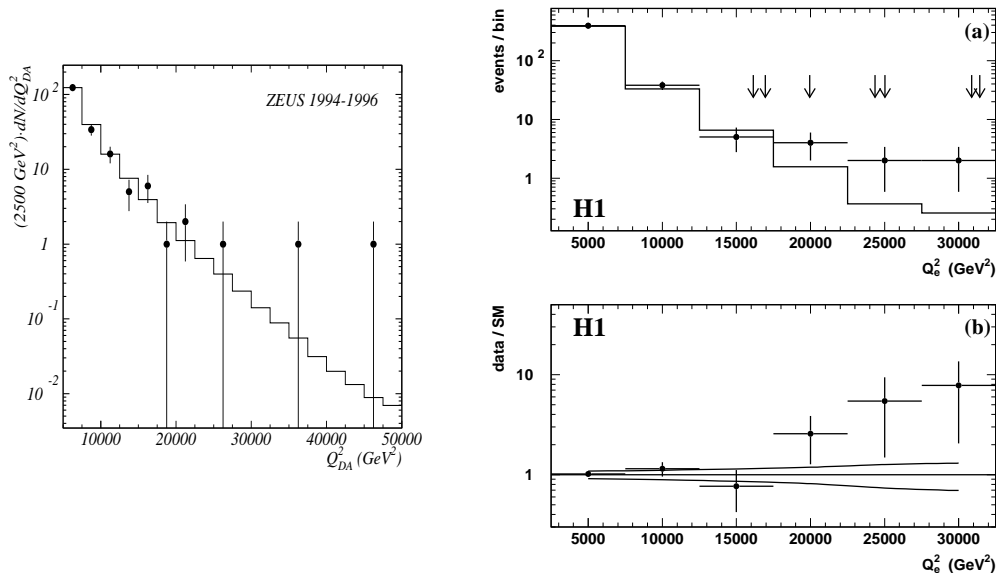


Figure 2: Q^2 dependences of events seen at high Q^2 , compared to standard QCD predictions (histograms), from ZEUS [19] (left) and H1 [20] (right). Subscripts DA (“double angle”) and e (“electron”) refer to experimental methods used in determining Q^2 .

The most popular interpretations described at the workshop rely either on a “conservative” approach, of descriptions by contact terms [21], or on more ambitious models with new particles, leptoquarks, possessing both baryon and lepton quantum numbers [22, 23]. The most promising of these models are based on supersymmetry, albeit in a somewhat variant form [23].

Contact terms are contributions to an effective Lagrangian, which describes the feed-down of very massive degrees of freedom to the standard model,

$$\mathcal{L}_{\text{contact}} = \sum_{\substack{i,j=L,R \\ q=u,d}} \frac{\eta_{ij}}{\Lambda_{ij}^2} \bar{e}_i \gamma_\mu e_i \bar{q}_j \gamma^\mu q_j, \quad (2)$$

with L and R referring to left- and right-helicities. These new terms are in direct analogy to the low-energy four-fermion description of the weak interactions. The parameters Λ_{ij} are new scales, most likely associated with heavy particle masses, typically in the TeV range. Generally, contact terms are not consistent with a “bump” in the mass distribution of the events, as marginally suggested by some of the H1 (but not ZEUS) presentations of the data.

In leptoquark descriptions, the events are due to one (or more) new states in the actual mass range of the events themselves, typically just above 200 GeV. Vector leptoquarks have larger cross sections than scalar, and can be excluded by results from the Tevatron [24]. Even for scalar leptoquarks, Tevatron bounds are strong. SUSY models are favored on this basis, because they result in suppressed branching ratios for the more readily observable leptonic decays.

Since the new particles are evidently produced singly rather than as particle-antiparticle pairs, candidate SUSY models cannot have the symmetry (“R-parity”)

built into many SUSY models precisely to forbid such single-superparticle production and decay mechanisms, and related (but avoidable) problems with proton decay [25]. In any case, the relevant terms in the Lagrangian are of the general form

$$\mathcal{L}_{\text{SUSY}} = \sum_{ijk} \lambda'_{ijk} L_i Q_j D_k, \quad (3)$$

which couples leptons (through the corresponding “superfield”) L_i , quarks through Q_j and the new superpartner, scalar leptoquarks, through D_k . Their coupling strengths are measured by the constants λ'_{ijk} , which must be determined from experiment. Bounds from various other experiments, including e^-p runs at HERA, limit the likely terms in Eq. (3) to one coupling e^+ with the d quark and a new scalar “squark” \tilde{c} , a superpartner of the charm quark [23, 26].

The impression left by the workshop is that the most common explanations of this excess *barely* escape many bounds derived from a wide class of other experiments. These events seem to have been born into a hostile world. Some bounds are from explicit searches in related experiments, most notably the Tevatron [24], where lower limits on masses at the 95% confidence level fall just short of the excess, in the 150-200 GeV^2 range for scalar leptoquarks, and seem to rule out vector leptoquarks altogether in this mass range. The Tevatron and LEP II [27] put lower limits on “contact terms” – signals of the exchanges of very heavy particles – in the few TeV range, which promise to grow larger. At the same time, very different, low energy precision experiments are equally, perhaps even more, restrictive. Of particular interest are the atomic parity-violation experiments, which, by a special serendipity, published new benchmarks of sensitivity within the few weeks prior to the conference [28]. Also striking are limits from searches for rare K decays and double beta decays [23].

Depending on the scenario chosen to account for the excess, these already-existing experiments closely circumscribe the range of parameters. This may be a good sign or bad, depending on what happens. What is exciting is that something must happen. H1 and ZEUS have already begun an anticipated doubling of statistics by the year’s end. Workers at the Tevatron advise us to “stay tuned”. If one of the favored explanations is correct, it is probable that signals will show up elsewhere soon, perhaps in events with pairs of high- E_T leptons and jets at the Tevatron, perhaps in rare K decays, perhaps in both.

Other, more and less conventional, explanations were also discussed, including a possible relation to the much debated high- E_T excess seen by CDF but (probably) not by D0. Such a connection is possible, although it might be expected to be larger, not smaller, in hadronic collisions [26]. Considered in isolation, it seems just possible that the excess is “simply” the sign of standard parton distributions that are a bit larger at $x \sim 1$ than in the present global fits [29]. Exotic color states were also suggested [30]. The adequacy of the “standard” calculation for the high- x region might be reexamined as well. One thing to keep in mind is that any increase in the QCD prediction would chip away at what is still a relatively small statistical discrepancy between theory and experiment, and would make a (perhaps disappointing) explanation in terms of a fluctuation more probable. Certainly, we were left with much to think over.

3 Perturbative QCD: DIS and Beyond, 1997

Now it's time to return to QCD, the primary theme of the conference. I will begin with a brief review of the theory that underlies the experiments described here, and then discuss results on the fundamental objects in perturbative QCD, structure functions and jet cross sections, along with parton distributions and the "BFKL" program. Most of the essential features of this wide range of topics must, of course, be found in the individual contributions to the workshop.

3.1 The Basics

The characteristic property of QCD is its asymptotic freedom, according to which the coupling $\alpha_s(\mu^2)$ becomes weaker as it is probed at shorter distances $1/\mu$. This extraordinary feature is exploited by identifying infrared (IR) safe quantities, cross sections (or other observables) which can be expanded as power series in α_s in terms of coefficients that are IR finite, and more generally independent of the light mass scales of the theory: Λ_{QCD} and the light quark and (vanishing) gluon masses. If an IR safe cross section depends on large scale Q and dimensionless kinematic variables x , it takes the schematic form

$$Q^2 \hat{\sigma}(Q^2, x) = \sum_{n \geq 0} c_n(Q^2/\mu^2, x) \alpha_s^n(\mu^2), \quad (4)$$

where the c_n are finite functions, or more often integrable distributions in the variable x . Classic examples of IR safe quantities are the total cross section for lepton pair annihilation to hadrons, and various jet and event shape cross sections in the same process.

The power of perturbative QCD (pQCD) for large classes of inclusive processes comes from its factorization and evolution properties. Factorization is expressed for unpolarized DIS of lepton ℓ on hadron h as

$$Q^2 \sigma_{\ell h}(q, p, m) = \sum_{\text{partons } i} \int_x^1 d\xi \hat{\sigma}_{\ell i} \left(\frac{Q^2}{\xi p \cdot q}, \frac{Q^2}{\mu^2}, \alpha_s(\mu^2) \right) \times f_{i/h}(\xi, \mu, m), \quad (5)$$

where q is the momentum transfer, $q^2 = -Q^2$, m represents the light scales of the theory (including the target mass $m = \sqrt{p^2}$), and the sum is over parton type i . The separation of the IR-safe partonic cross section $\hat{\sigma}_{\ell i}$ from the nonperturbative, but universal, parton distribution $f_{i/h}$ requires a factorization scale, μ , usually identified with the renormalization scale at which the coupling is evaluated. The physical cross section, of course, is independent of μ . Corrections to (5) are *power suppressed*, by at least $1/\mu^2$, so that when μ is chosen to be of order Q , factorization in terms of parton distributions is a very good approximation at large momentum transfer. On the other hand, as Q^2 decreases below the proton mass, we may expect "higher-twist" power corrections to come into play.

Each of the DIS structure functions F_i , $i = 1, 2, 3$ satisfies a factorized form like Eq. (5). The convolution in parton fractional momentum ξp is conveniently denoted as, for instance,

$$F_2 = C_2 \otimes f, \quad (6)$$

with C_2 an IR safe ‘‘coefficient function’’, analogous to $\hat{\sigma}$ in Eq. (5). Our freedom to choose μ in the factorized DIS cross section,

$$\mu \frac{d\sigma}{d\mu} = 0, \quad (7)$$

readily leads to the DGLAP evolution equations [31], by separation of variables,

$$\begin{aligned} \mu \frac{d\hat{\sigma}}{d\mu} &= -\hat{\sigma} \otimes P(\alpha_s), \\ \mu \frac{df}{d\mu} &= P(\alpha_s) \otimes f, \end{aligned} \quad (8)$$

where the P 's are the familiar evolution kernels of QCD. They are perturbatively calculable precisely because $\hat{\sigma}$ is. Like the factorization formula, the evolution equations are valid up to corrections suppressed by $1/\mu^2$.

Written out in terms of DGLAP kernels P_{ij} , the evolution equations are

$$\mu^2 \frac{\partial}{\partial \mu^2} \begin{pmatrix} q(x) \\ G(x) \end{pmatrix} = \frac{\alpha_s(\mu^2)}{2\pi} \begin{pmatrix} P_{qq} & P_{qg} \\ P_{gq} & P_{gg} \end{pmatrix} \otimes \begin{pmatrix} q(x) \\ G(x) \end{pmatrix} \quad (9)$$

for singlet distributions, and

$$\mu^2 \frac{\partial}{\partial \mu^2} q_{\text{NS}} = \frac{\alpha_s(\mu^2)}{2\pi} P_{qq} q_{\text{NS}} \quad (10)$$

for nonsinglet. These, along with a set of boundary conditions, are used to predict parton distributions and structure functions for previously unmeasured values of Q^2 . (We should note that DGLAP evolution alone does not allow us to ‘‘evolve’’ in x ; more on this below.)

A result of this past year deeply rooted in DGLAP evolution is the high-statistics determination of α_s , reported by CCFR through analysis of the evolution of F_2 and F_3 [32], using the proportionality of the logarithmic derivative with respect to Q^2 of these structure functions to $\alpha_s(Q^2)$. With this result, $\alpha_s(M_Z^2) = 0.119 \pm .002$, measurements of the strong coupling from relatively low-energy DIS experiments have come (predominantly, if not completely [33]) into agreement with values found from e^+e^- annihilation at the Z mass. This has put to rest some of the speculation based on discrepancies between the two ranges of energy. Not all DIS estimates give such a high value, however, although scaling violation in F_3 appears to be the most precise.

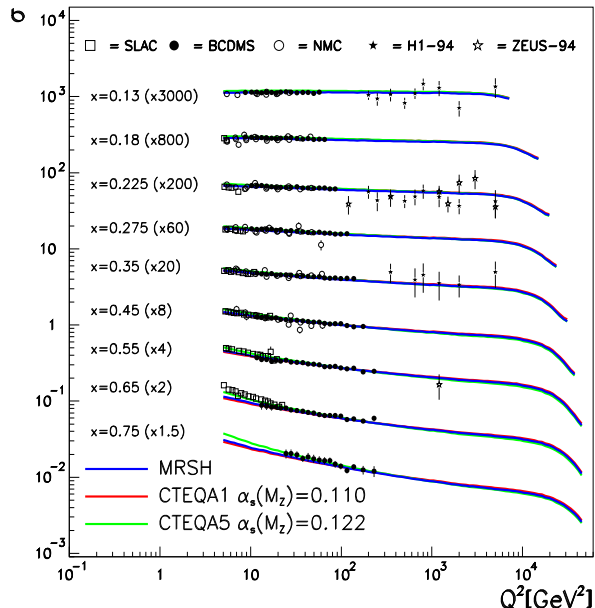


Figure 3: (a) H1 fit to high- Q^2 neutral current cross section approximately normalized to F_2 at low energies [7].

3.2 Structure Function Measurements

ZEUS and H1 presented data, and new analyses of data, from 1994 through 1996, mapping out the behavior of F_2 over an increasing range of x and Q^2 , with shrinking errors [14, 34, 35]. The primary emphasis was on the very high- Q^2 and very low- Q^2 results. These were complemented by the final NMC results for Deuterium, at large x and moderate Q [1], and those from CCFR [2].

The high- Q^2 analysis at HERA became possible as the integrated luminosity passed 20 pb^{-1} by the end of 1996. We have already discussed the observed excess of events in that region. A feeling for the nature of the DGLAP-based evolution of the neutral current cross section to large Q^2 is given by Fig. 3, which plots the cross section of Eq. (1) scaled by the coefficient of F_2 . On the basis of analyses such as these, H1 and ZEUS have estimated uncertainties in the NLO predictions at high Q^2 of order ten percent [36].

New low x and Q^2 results from HERA were made possible by runs with detector modifications and/or shifts in the event vertex, which extend coverage of the existing detectors to more forward regions [34, 35]. Figs. 4 and 5 show, respectively, trends of the data with Q for representative values of x and vice-versa.

As Fig. 4 shows, charm production plays a large role in the total cross section for small x even for relatively small Q^2 , comparable to the charm mass [37, 38]. This is understandable; the relevant variable is now $W^2 \sim Q^2/x$ at small x , and we can be far above the charm threshold even for $Q < m_c$, if x is small enough. Indeed, charm production is an important effect even for photoproduction, where $Q^2 = 0$ [39].

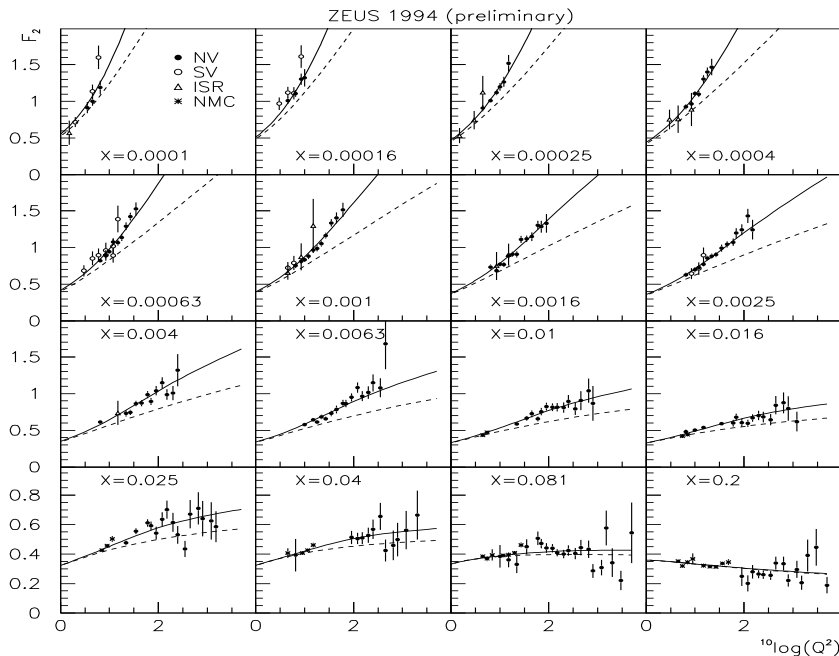


Figure 4: Q -dependence of F_2 for representative x at low Q [36]. The solid curve is a fit, the dashed curve omits the charm contribution.

The special interest of low Q comes in part from the very success of DGLAP evolution in describing F_2 to surprisingly low values of Q^2 , even below 1 GeV^2 . The GRV parton distributions [40] are based on “valence-like” boundary conditions in this range, and give a reasonable description of F_2 there. Below $Q^2 \sim 1 \text{ GeV}^2$, deviations begin to show up, in which the cross section grows less rapidly toward small x , corresponding to a slow-down of evolution compared to perturbative predictions. The picture here remains a bit cloudy, with various explanations, fits [41] and models offered, often inspired by pre-QCD phenomenology, such as vector meson dominance [42] and Regge theory [43], alongside efforts at quantitative prediction based on the perturbative BFKL formalism [44], which itself has one foot in QCD perturbation theory and one in Regge theory. The transition region between perturbative and nonperturbative degrees of freedom is not wide, at least as measured in GeV, but no single model can yet bridge it. We must hope for theoretical developments in this direction, a question to which we shall return.

In terms of pQCD itself, we can identify two generic corrections for low x and Q not included in the DGLAP equation at NLO, which warn us of the transition region. These are: logarithms of x at higher orders in the splitting kernel, and power corrections that are order $1/\mu$ with $\mu \sim Q$ the factorization scale. It is important to emphasize that these corrections are different. In particular, the former are consistent with leading twist factorization, the latter require (at the least) generalized factoriza-

ZEUS 1995

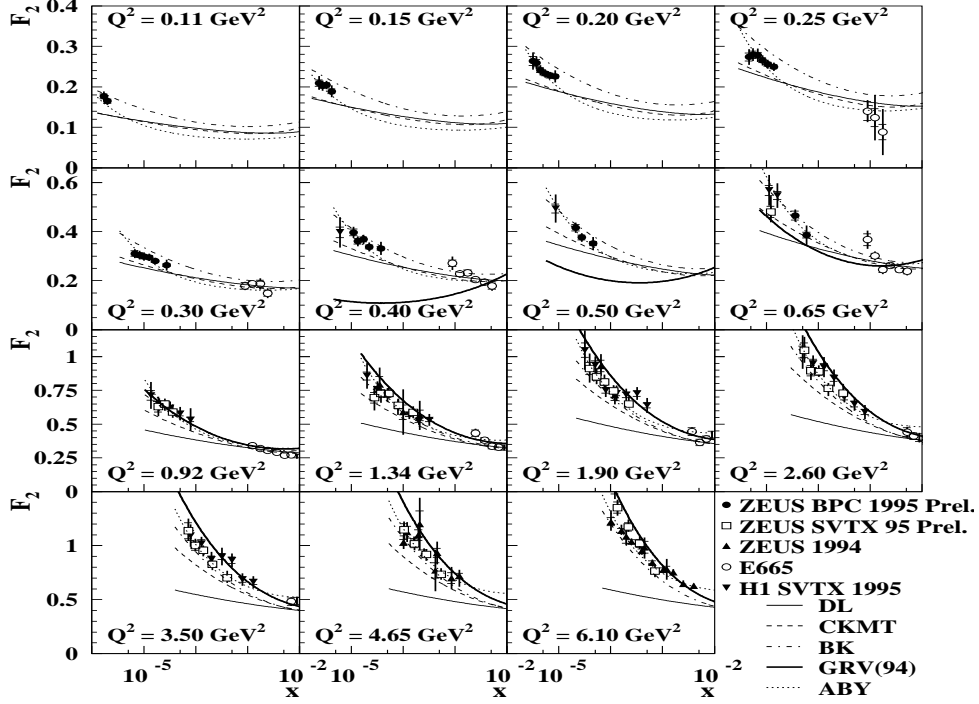


Figure 5: x -dependence of F_2 for low Q^2 [35].

tions. The BFKL equation deals with logarithms of x at leading power. Let's review how it arises in DIS.

3.3 The BFKL Program: Theory and Experiment

The well-known BFKL equation [45], applied to DIS, summarizes leading logarithms in x . Let me reemphasize that the BFKL equation is fully consistent with DGLAP evolution, and constitutes a reorganization of information in the DGLAP kernels P . Like the DGLAP equation, it may be derived from a factorization of DIS structure functions, but now one that is accurate only to the level $1/\ln(x)$,

$$\begin{aligned}
 F(x, Q^2) &= \int_x^1 \frac{d\xi}{\xi} C\left(\frac{x}{\xi}, \frac{Q^2}{\mu^2}\right) G(\xi, Q^2) + \mathcal{O}(1/Q^2) \\
 &= \int d^2 k_T c\left(\frac{x}{\xi'}, Q, k_T\right) \psi(\xi', k_T) + \mathcal{O}(1/\ln(1/x)) . \quad (11)
 \end{aligned}$$

In the second form, the wave function ψ is in a k_T convolution with the coefficient function, while the fractional momentum ξ' plays the role of a factorization scale.

The relation of ψ to the gluon distribution G is

$$G(\xi, Q^2) = \int^Q d^2k_T \psi(\xi, k_T). \quad (12)$$

Just as the first factorization form leads to DGLAP evolution by invoking the independence of F on μ , so the independence of F on ξ' leads to another evolution equation, analogous to Eq. (8), but now with a convolution in transverse momentum rather than ξ' . This is the BFKL equation [45],

$$\xi \frac{d\psi(\xi, k_T)}{d\xi} = \int d^2k'_T \mathcal{K}(k_T - k'_T) \psi(\xi, k'_T). \quad (13)$$

The kernel \mathcal{K} turns out to be independent of ξ in this approximation, although by dimensional analysis it could have depended upon it.

Further insight into the significance of the BFKL equation can be found in the very general “Wilsonian” treatment [46] of the underlying factorization, by separating the dynamics into independent Hamiltonians, appropriate to the opposite-moving external particles. I think we can anticipate progress in interpreting other factorizations from this approach in the coming years.

Solutions to the BFKL equation may be found by substituting trial solutions in the form of powers of ξ and k_T . These solutions take a continuous range of powers of ξ , of which the most singular is the famous BFKL result,

$$\xi \psi(\xi, k_T) \sim \xi^{-4N \ln 2(\alpha_s/\pi)}. \quad (14)$$

The scale, and therefore the size, of α_s is undetermined in this leading logarithm formalism. In addition, the full description of near-forward scattering at next-to-leading logarithm in x requires three-gluon exchange contributions, which are not included in the BFKL equation at all. These cautions aside, a provocative treatment of nonleading logarithms in solutions to the BFKL equations based on analogy to DGLAP evolution was presented [47].

From the DGLAP point of view, the BFKL equation sums up those contributions to the gluon-gluon splitting function that are leading at each order in α_s , of the form $\alpha_s^n [\ln^{n-1}(1/x)]/x$. It is by now an old story, however, that the growth in F_2 at low x should not be interpreted as a direct observation of unadorned BFKL dynamics. NLO DGLAP evolution seems quite up to the task, and the higher orders seem not to be needed.

In any case, the solution Eq. (14) cannot strictly speaking be exact, because it predicts a gluon distribution that increases as a power of x , and therefore a total cross section that increases as a power of $W^2 \sim 1/x$, which would eventually violate unitarity bounds. One way of understanding this behavior is that power-like solutions do not build in momentum conservation, which is only enforced at the level of nonleading logarithms.

At the same time, when x is small enough that $\alpha_s \ln(1/x) \sim 1$, nonleading logarithms must be taken into account, and have the effect of moderating the growth of $G(x)$ with $1/x$. This general picture is consistent with what we have seen above,

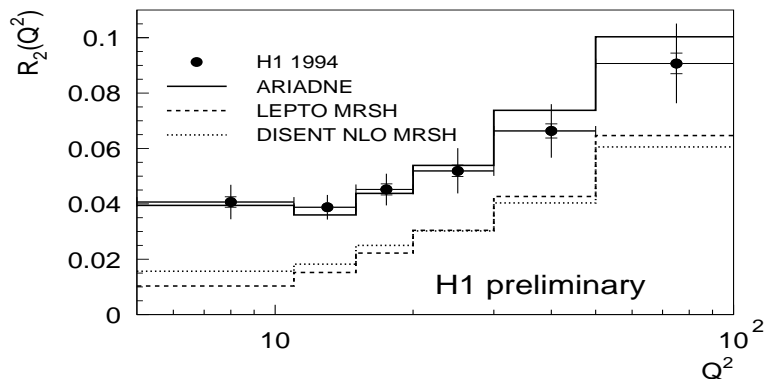


Figure 6: $R_2 \equiv (N_{2\text{ jet}}/N_{\text{all}})$ measured by H1 [7], compared to NLO calculations and ARIADNE.

in Fig. 5, for instance, but there is no assurance that by the time resummed BFKL logarithms become important for structure functions, a perturbative treatment is appropriate at all. Nevertheless, it is possible to construct models for $\psi(x, k_T)$, based on the evolution equations we have encountered above, and to derive in this way a fairly good picture of low- x and Q^2 evolution [44].

The search for BFKL phenomenology, that is, for experiments whose interpretation requires the resummation of logarithms of $1/x$, has by and large shifted from the structure functions to less inclusive measurements, following general lines introduced by Mueller and Navelet [48] in hadron-hadron scattering. The method is to identify events that can be “tagged” by jets at wide rapidity separations. If the transverse momentum of the jets is substantial, there is little chance of a higher- p_T jet in between, and DGLAP evolution should be unimportant. At the same time, if the partonic fractions of the two jets are very different, perturbative BFKL dynamics ought to dominate. At *very* high energy, the solution (14) would describe such cross sections, with $\ln(1/\xi)$ replaced by the rapidity difference between the two jets. Energy conservation, however, makes it impossible to have enough gluons emitted between the tagged jets to reproduce the exponential of the rapidity, and more sophisticated numerical approaches appear to be necessary. Among these are very new BFKL “Monte Carlo” generators [49]. The general features of BFKL evolution have been built into the event generator ARIADNE, at a somewhat less formal level.

Studies searching for such BFKL effects have been carried out at the Tevatron [50] in terms of angular correlations between the tagged jets, without showing specifically BFKL behavior. At the same time, studies of dijet cross sections by ZEUS [51] at large rapidity separations are more encouraging, at least when ARIADNE is compared to NLO calculations [52]. A corresponding example from H1 is shown in Fig 6. The difference between the two reports may be more apparent than real, however, since the “theory” used in each case is different.

Finally, progress has been reported in the extension of the BFKL equation. The program of Fadin and Lipatov toward the calculation of the two-loop kernel for the BFKL equation, appears to be at the threshold of completion [53]. The capstone

of this enterprise, the “two-region-two-gluon vertex”, has been presented at this workshop for the first time. The expression remains at this time a bit unwieldy to speculate on its quantitative consequences, although expected signs of the running of the coupling are possible to pick out. Alternative technical approaches, based on helicity methods are also being pursued [54].

3.4 Direct Evolution for Structure Functions

To incorporate the extra information on evolution of DIS structure functions contained in the BFKL equation, while still keeping logarithms of Q , it is useful to *demand* an evolution that is independent of changes of factorization scheme, up to unincorporated corrections in $\ln(1/x)$ as well as $\ln Q^2$. The latter are taken care of by DGLAP evolution. The former may be incorporated by studying the evolution of the structure functions themselves [55]. Combining factorization

$$F_2^{\text{NS}}(Q) = C\left(\alpha_s(Q^2)\right) \otimes q_{\text{NS}}(Q) \quad (15)$$

with the nonsinglet evolution equation (10), we readily derive an evolution equation for the nonsinglet structure function itself,

$$\frac{\partial}{\partial \ln Q^2} F^{\text{NS}}(Q) = \left(\frac{\partial \ln C}{\partial \ln Q^2} + C \otimes P_{qq} \otimes C^{-1} \right) \otimes F^{\text{NS}}(Q) \equiv \hat{\Gamma}_{\text{NS}} \otimes F^{\text{NS}}, \quad (16)$$

in which $\hat{\Gamma}_{\text{NS}}$ includes the evolution dependence of the coefficient function through the running coupling. The extension to singlet structure functions follows the same pattern.

This formulation makes possible a “consistent”, “scheme-independent” treatment of logarithms of x , through the incorporation of coefficient functions, along with evolution in Q^2 . As evolution proceeds, the input level of accuracy in $\ln x$ and $\alpha_s(\mu)$ are retained, by avoiding scheme-dependent complications which can arise from separating the coefficient functions from the parton distributions. This makes possible surprising improvements in the fit to the low- x HERA data [55].

Interestingly, the same general approach can be used a very high x , to take into account logarithms of $1-x$ not included in NLO [56]. In this case, the nonsinglet evolution equation alone is adequate, as logarithms of $1-x$ do not involve flavor mixing. The equation that takes into account these corrections is exactly Eq. (16), in terms of DIS scheme quark distributions and a resummed coefficient function $C(x)$. The logarithms of $1-x$ are generated from moments, $\tilde{C}(N) = \int_0^1 dx x^{N-1} C(x)$. $\tilde{C}(N)$ is known in an explicit form in which all leading and next-to-leading logarithms are exponentiated [57]

$$\tilde{C}(N, \alpha_s(Q)) = \exp \left[-C_F \int_0^1 dz \frac{z^{N-1} - 1}{1-z} \int_{(1-z)}^1 \frac{d\eta}{\eta} \frac{\alpha_s(\eta Q^2)}{\pi} + \dots \right]. \quad (17)$$

Evolved according to Eq. (16), the DIS scheme distributions, whose sum is the structure function in this limit, will be enhanced compared to the result found by evolving either $\overline{\text{MS}}$ or DIS distributions according to NLO DGLAP evolution alone.

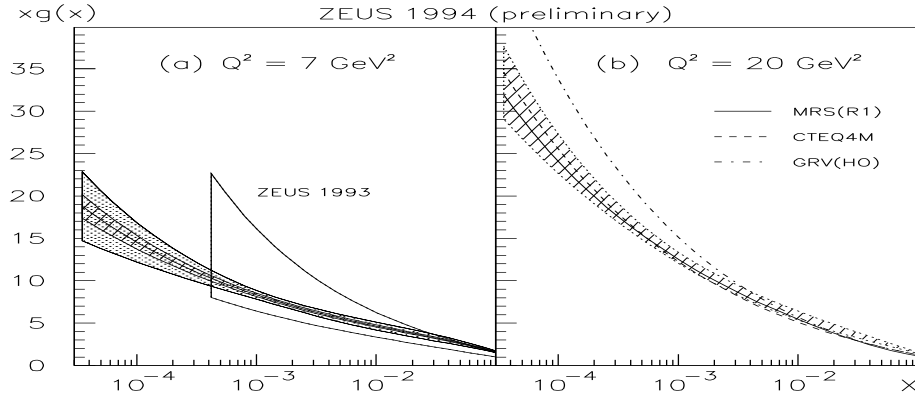


Figure 7: The gluon distribution fit of ZEUS, from [36].

3.5 Parton Distributions and Charm

An analysis directly in terms of structure functions, however useful for inclusive DIS, is limited to that process. To treat jet cross sections, or heavy quark production in DIS and other processes, we need to retreat from the ascetic evolution in terms of observables only, to parton distribution functions. Then, the generic cross section is of the form

$$\sigma_{hh'} = \sum_{\text{partons } ij} f_{i/h} \otimes f_{j/h'} \otimes \hat{\sigma}_{ij}, \quad (18)$$

where $\hat{\sigma}$ is an IRS distribution, calculable in pQCD.

The gluon distribution can be determined by fitting F_2 at NLO [36], and is also accessible at leading order in jet, heavy quark and direct photon cross sections [58, 59, 60, 61]. An example of the former is shown in Fig. 7 from [36], which exhibits a good agreement with results of the global fitting programs of MRS [62] and CTEQ [63]. The more exclusive determinations, such as those based on direct photons, are appealing because the gluon distribution enters them at leading order. At the same time, higher-order corrections are generally more difficult to control in these cases, and sometimes effects that are formally nonleading twist, such as “intrinsic” parton momenta, are important [64, 65]. Indeed intrinsic transverse momenta of order 1 GeV seem necessary to explain the comparison of NLO theory with experiment for direct photon production measured by the fixed target experiment E706, as illustrated by Fig. 8. Non-NLO effects of this type should be anticipated in any single-particle inclusive or related measurement.

Such considerations also arise in connection with the program of measuring parton distributions for photons through “resolved” photoproduction experiments. Partons are associated with dijets, whose rapidities and transverse momenta η_i and E_{T_i} are related to an equivalent partonic fraction,

$$x_\gamma = \frac{1}{2yE_e} \left(E_{T1} e^{-\eta_1} + E_{T2} e^{-\eta_2} \right). \quad (19)$$

E706 π^- Be at 515 GeV

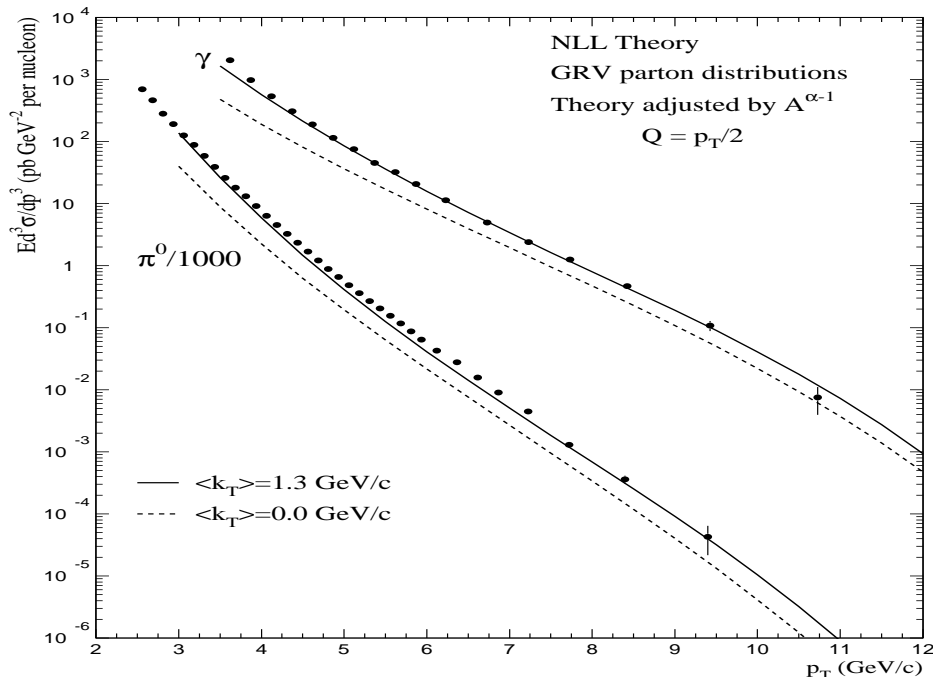


Figure 8: Direct photon and π^0 inclusive cross sections measured by E706 [64].

The observation of Rutherford-like cross sections for “resolved-enriched” $x_\gamma < 1$ in jet photoproduction has demonstrated the feasibility of such determinations [66, 67], and the characteristic evolution of the quark distribution has been observed. Recent measurements, however, show enhancements in the resolved region (Fig. 9) which seem to be due to multiple interactions [11, 68]. Such interactions are also “higher twist” – formally power-suppressed in p_T . Again, a fuller understanding of such non-NLO effects will be necessary in these cases.

A better-understood, but still challenging issue is the role of charm in DIS. We have already seen that the charm structure function F_2 is a substantial part of the total (see Fig. 4). In response to this new data, 1997 has become the year of quark masses in parton distributions [69, 70, 71, 72]. The problem here is to develop a treatment that is at once self-consistent, and accurate, when parton distributions are evolved through $\mu \sim m_c$, where m_c is the charmed (or other) quark mass, $m_c \gg \Lambda_{\text{QCD}}$.

We note first that since $m_c \gg \Lambda_{\text{QCD}}$, it is perfectly acceptable to treat the c quark as perturbatively generated, and to work throughout in a “three-flavor” scheme, for which the *only* quark distributions are $u(x)$, $d(x)$ and $s(x)$. This is a self-consistent approach up to order Λ_{QCD}/m_c , but it suffers from (at least one) serious drawback. For scales $Q \gg m_c$, we must be willing and able to compute very high-order diagrams in which c -quark pairs are produced, or be prepared to lose lots of terms that behave as $\alpha_s^m(Q^2) \ln^m(Q/m_c)$ in the coefficient functions in Eq. (6). This problem becomes worse and worse at small x , since the phase space available for c -pair production is

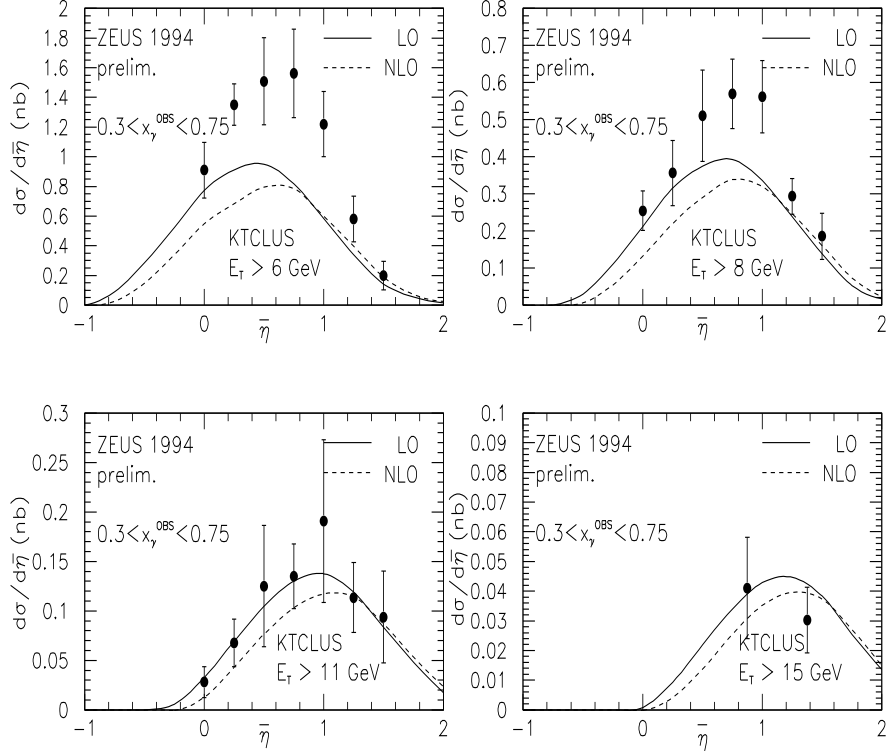


Figure 9: Cross sections for photoproduction of dijets in various ranges of x_γ [11].

measured not by Q^2 , but by $W^2 = Q^2(1-x)/x$.

The provisional solution to these problems adopted by the global fits until recently was to take the c quark into account by ignoring it for $\mu < m_c$, and treating it as massless for $\mu > m_c$, switching from a three- to a four-quark fit at that point. Clearly, this is only a rough picture of the relevant physics.

A much more appealing approach is to absorb powers of $\ln(Q/m_c)$ into the evolution of the c quark distribution,

$$\frac{\partial}{\partial \ln \mu^2} f_c(\mu) = \frac{\alpha_s}{2\pi} P_{qq} \otimes f_c(\mu). \quad (20)$$

As described in [69, 72], the kernel P is the standard $\overline{\text{MS}}$ kernel, a result that follows by showing that it is possible to construct a factorized expression for the cross section

$$\sigma(Q, m_c) \sim \hat{\sigma}(Q/\mu, m_c/\mu) \otimes f_c(\mu), \quad (21)$$

in which the hard-scattering function obeys

$$\hat{\sigma}(Q/\mu, m_c/\mu) = \hat{\sigma}(Q/\mu, 0) + O(m_c/\mu), \quad (22)$$

so that, as above,

$$\frac{\partial}{\partial \ln \mu^2} \hat{\sigma} = -\hat{\sigma} \otimes P^{\overline{\text{MS}}}. \quad (23)$$

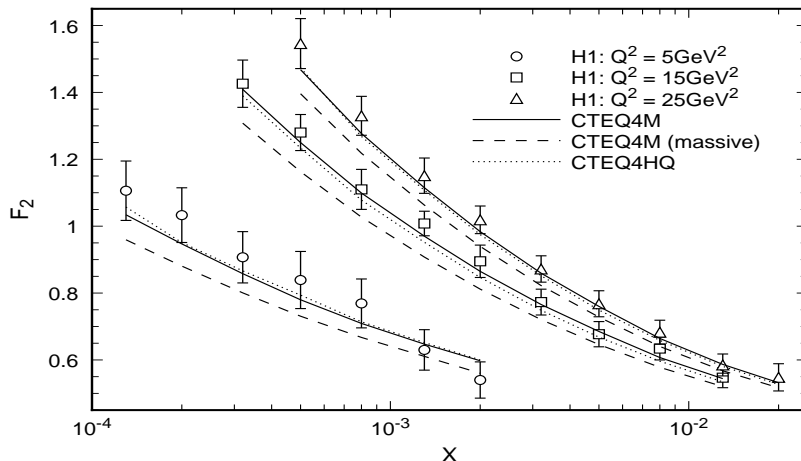


Figure 10: Fits of H1 measurement of F_2 using the (old, massless) CTEQ4M fits, with and without quark masses in the coefficient function, and the variable flavor fit CTEQHQ.

The result of a new CTEQ fit [69, 71], employing this scheme, is shown in Fig. 10. These, and related [70], “variable flavor schemes” seem to be demanded for a full description of the small- x DIS data, and correspondingly for applications in hadron-hadron scattering. This year has seen truly significant progress in this direction.

3.6 QCD at NLO and NNLO: How Much Can We Expect?

QCD predictions based on factorization, next-to-leading order calculations and parton distributions run the gamut from spectacular success to egregious failure. An example of recent success is found in jet cross sections at the Tevatron, at least up to transverse momenta of 200 GeV [73], while a particularly interesting recent failure is in the ratio of W cross sections with and without a single jet [74].

All other things being equal, NLO predictions work best when all scales are comparable. Thus, top production is easier to handle than bottom production at the Tevatron, while DIS at x of order unity is better described at NLO than when $x \rightarrow 0$. Similarly, steeply falling cross sections are sensitive to nonperturbative k_T and/or transverse momenta from high orders (see Fig. 8 above). Finally, any edge of phase space, even p_T^{max} , is dangerous. For example, the default power suppression in DIS is $1/[(1-x)Q^2]$, and similarly for fragmentation, an effect that may be at the basis of the rise in octet contributions to ψ production at $z \rightarrow 1$ [75].

We should note, however, that our expectations for success have become more demanding, and our recognition of failure more ready. This is due in large part to the accumulation of NLO calculations [76], first for electroweak processes, such as Drell-Yan and DIS, for direct photon, heavy quark and jet production in hadronic collisions [77], and for jet production in DIS [52] and e^+e^- annihilation [78]. Certainly, next-to-next-to-leading-order calculations can lead to further improvements, although except

when all relevant scales are very large, power corrections can be competitive with NNLO.

Prospects for improved partonic calculations were extensively discussed at the workshop. Certain very basic quantities, such as the QCD beta function in certain gauges, and the first moment of the polarized-DIS structure function $g_1(x)$ already can be computed to four (!) loops [79]. More generally, the use of still-new techniques of supersymmetry and strings are pointing the way toward two, and even higher, loop amplitudes in QCD. The status of these calculations is, perhaps, similar to that of NLO calculations in the late 70's. Time will tell if the technology of two loops can reach the sophistication, and phenomenological impact, of the NLO calculations that grew out of the pioneering efforts of that time.

The string approach, employed originally to calculate massless one-loop QCD helicity amplitudes [80], has been largely superseded by methods based on judicious use of SUSY, for instance, by expressing QCD amplitudes as linear combinations of amplitudes in theories with four supersymmetries (“ $N = 4$ ”) and one supersymmetry (“ $N = 1$ ”), combined with clever decompositions of color amplitudes. The overall program has been labelled “total quantum number management”. The most striking simplification [81], however, is based on a very old idea, that loop amplitudes may be constructed iteratively using “cutting rules”, which specify the discontinuities of Feynman diagrams as products of amplitudes and complex conjugates found simply by dividing the diagrams in two. At the same time, progress was reported on deriving – in principle – QCD amplitudes at *arbitrary* loops, by a new approach to string techniques [82]. The practicality of these new techniques, of course, is undemonstrated, but their potential is great.

4 Other Factorizations: New Densities, New Evolutions

The value of the factorization of long- from short-distance dynamics goes far beyond unpolarized structure functions and related hard-scattering cross sections. This year has shown, not only applications to polarized structure functions, but also the extensions of the general method of factorization to less inclusive final states. The value of an extension of the factorization program depends upon the experimental, as well as theoretical accessibility of the relevant cross section.

4.1 The Sibling Distributions: Polarized DIS

Inclusive polarized parton distributions are at the next level of hadron structure from the unpolarized distributions discussed above. They are “siblings” of unpolarized distributions, in the sense that they were part of the parton model analysis of DIS.

Their analysis begins with the hadronic tensor for polarized DIS,

$$\frac{d^2\sigma}{d\Omega dE} = \frac{\alpha_{\text{EM}}^2}{2mQ^4} \frac{E_e}{E'_e} L^{\mu\nu} W_{\mu\nu}$$

$$\begin{aligned}
W_{\mu\nu} &= W_{\mu\nu}^{\text{unpol}} + \frac{i}{E_e - E'_e} \epsilon_{\mu\nu\lambda\sigma} q^\lambda s^\sigma g_1(x, Q) \\
&\quad + \frac{i}{(E_e - E'_e)^2} \epsilon_{\mu\nu\lambda\sigma} q^\lambda [p \cdot q s^\sigma - s \cdot q p^\sigma] g_2(x, Q), \tag{24}
\end{aligned}$$

with s the nucleon spin. From the polarized structure functions g_1 and g_2 , we abstract polarized parton distribution functions, for instance

$$g_1(x, Q) = \frac{1}{2} \sum_f e_f^2 \Delta q_f(x, Q) + O(\alpha_s), \tag{25}$$

where Δq is $q_f^+ + \bar{q}_f^+ - q_f^- - \bar{q}_f^-$, the difference between the total positive helicity and negative helicity contributions of quarks and antiquarks of flavor f . At higher orders, the gluon begins to contribute as well. The study of polarized parton distributions allows us to address in parton language the question of what carries the proton spin.

Polarized distributions enjoy the same pattern of factorization and evolution [83, 84, 85] as unpolarized distributions, may be combined with NLO calculations [86, 87, 88, 89], and may be studied in the same manner for their small- x behavior [90].

Within the past two years, efforts have accelerated to determine polarized parton distributions [86, 87, 17]. The very recent E154 results for g_1^n (Fig. 11) will play an enduring role. They are also significant in improving estimates of the neutron contribution to one of the best-computed predictions of QCD, the Bjorken sum rule,

$$\int_0^1 (g_1^p(x) - g_1^n(x)) dx = \frac{1}{6} \left| \frac{g_A}{g_V} \right| \left(1 + \sum c_n \alpha_s^n \right), \tag{26}$$

with the c_n known out to c_3 . Kinematics, however, restricts the data to a relatively limited range in x . At the same time, since g_1 is decreasing rapidly as $x \rightarrow 0$, theoretical estimates of its behavior in this limit [90] will become more important as the data becomes more precise in the accessible region [91]. Of course, should HERA itself become a polarized collider [92], we will be able to test these predictions.

Another important current in polarized DIS is semiinclusive asymmetries, which have been pioneered by SMC [93, 94], and are now being pushed forward by HERMES [95]. Especially interesting will be studies of polarized charm production, since it probes the polarized gluon distribution at leading order. The caveats mentioned in the previous section, associated with determining parton distributions in non-inclusive scattering measurements, apply here as well, of course. Certainly, it will be important to complement measurements of this sort with those from the analysis of evolution for inclusive structure functions [84], and with the experiments promised at a polarized RHIC.

4.2 Extended Polarization Analysis; DVCS

The parton distribution function $q(x)$ may be interpreted as the expectation value of the number operator in nucleon state $|p\rangle$,

$$q(x) = \int d\ell \langle p | b_q^\dagger(xp + \ell) b_q(xp + \ell) | p \rangle, \tag{27}$$

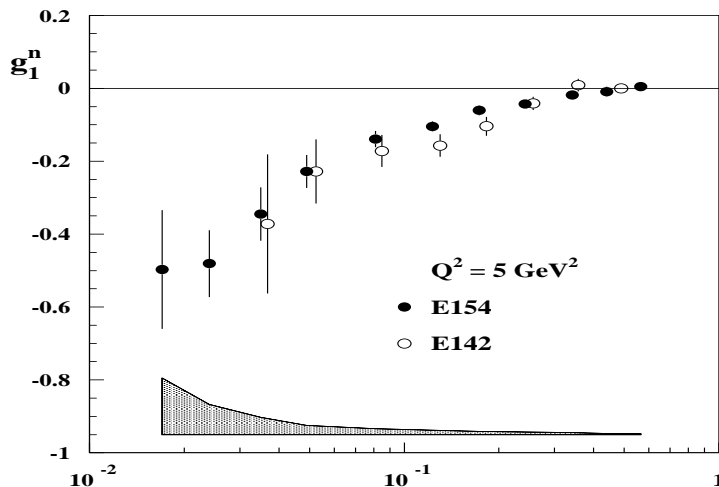


Figure 11: Final E154 results for g_1^n [4].

at fractional momentum x , integrated over the other momentum components, which we denote by ℓ . The first moment of such a parton distribution,

$$p_0 \int_0^1 dx x q(x) \quad (28)$$

is then the contribution of quark q to the total momentum of the nucleon. It is, however, not possible to quantify contributions to angular momentum in this fashion.

One of the developments of the preceeding year is the introduction of a class of “asymmetric” parton distribution functions [96, 97], in part to create a partonic language with which to discuss orbital angular momentum, and in part to discuss diffractive vector boson production, to which we will turn shortly. An asymmetric parton distribution may be thought of as a matrix element of the form

$$Q(x, x - \delta) = \int d\ell \langle (1 - \delta)p | b^\dagger((x - \delta)p + \ell) b(xp + \ell) | p \rangle. \quad (29)$$

Ji [98] has shown that expectations of this kind are naturally interpreted in terms of partonic contributions to angular momentum, and also that the relevant matrix elements are available for study in what he called deeply virtual Compton scattering (DVCS), $p + \gamma^*(Q) \rightarrow p' + \gamma$, the exclusive process in which an off-shell photon scatters on-shell by exchanging momentum with a proton. The appropriate limit for extracting $Q(x, x')$ is one in which the momentum transfer to the proton is mostly longitudinal, so that the proton essentially “slows down” a little bit in the center of mass frame. The observability of this process is under study, and beyond that questions of evolution and universality may be raised. Indeed, as observed above, there is a close relation of DVCS to the constellation known as diffractive phenomena. In DVCS an on-shell photon is produced diffractively. Let us now turn to the diffractive production of hadrons.

4.3 Diffraction

In discussing diffraction, it is worthwhile to keep in mind the distinction between leading and nonleading *twist*. Although it has a more exact technical definition, in DIS the term *twist* can be used simply to identify the power behavior of a given partonic contribution in the momentum transfer Q , leading twist for leading power in Q , and nonleading twist for nonleading power of Q . All the standard unpolarized parton distributions enter at twist equal to two. It is possible to extend the parton model in perturbative QCD, to include short-distance reactions that are initiated by *more than one parton*.

In the standard parton model picture, we compute cross sections that are the square of an amplitude for the hard scattering of a single parton. At nonleading twist, we must consider the possibility of interference between the amplitude for the hard scattering of a single parton with the amplitude for the scattering of two partons (twist three), or the square of the two-parton scattering amplitude (twist four). In general, the twist of such contributions is the number of partons in the amplitude plus the number in the complex conjugate amplitude. As we shall see, diffractive processes occur at both leading and nonleading twist.

A diffractive DIS process is of the general form $p + \gamma^* \rightarrow p' + X$, for hadronic final state X where $t = (p - p')^2$ is small. Since the proton is present in both the initial and final states, the production of X involves no transfer of quantum numbers. A typical signature for diffraction is a gap in rapidity between the proton and the particles that make up X , but this is not strictly necessary. When t is small, convenient kinematic variables are (as usual $W^2 = (p + q)^2$)

$$\begin{aligned} x_{\mathcal{P}} &= \frac{M_X^2 + Q^2}{W^2 + Q^2} \\ \beta &= \frac{Q^2}{2x_{\mathcal{P}}p \cdot q} = \frac{Q^2}{M_X^2 + Q^2} \\ \Rightarrow \beta x_{\mathcal{P}} &= x = \frac{Q^2}{2p \cdot q}, \end{aligned} \tag{30}$$

where $x_{\mathcal{P}}$ is the fraction of longitudinal momentum lost by the proton. The variable β is an equivalent “partonic fraction” for the production of the final state X from the collision of an object of momentum $x_{\mathcal{P}}p$ with the photon γ^* . Since the exchange of momentum to the photon is free of quantum numbers, it is often thought of as carried by the “pomeron”, a hypothetical object whose exchange is thought to dominate elastic scattering between hadrons at fixed momentum transfer and very high energy (the Regge limit).

In terms of these variables, it is conventional to define a four-fold differential cross section, which can be measured if the momentum of the final-state proton is actually observed.

$$\frac{d^4\sigma}{dQ^2 d\beta dx_{\mathcal{P}} dt} = \frac{2\pi\alpha_{\text{EM}}^2}{\beta Q^4} (1 + (1 - y)^2) F_2^{D(4)}, \tag{31}$$

A triply-differential distribution is found by integrating over t .

Experiments that observe diffraction may be inclusive or exclusive. Inclusive diffractive DIS, like inclusive DIS, may be initiated by a single parton; the soft partons that carry color into the final state are not observed. In view of our observations above, inclusive diffraction is expected to be leading twist and thus leading power in momentum transfer, and indeed F_2^D scales in the same manner as the full F_2 [99, 100].

These considerations suggest a separate factorization for diffractive processes, analogous to Eq. (6),

$$F^D = \sum_{\text{partons } i} C'_i \otimes f_i^D \quad (32)$$

with f_i^D a diffractive parton distribution for parton i [101, 102], defined by the restriction that the final state include a forward proton. If this relation holds, we may expect to derive evolution equations for diffractive as for fully-inclusive DIS. On the other hand, it is not at all clear that diffractive parton distributions are “universal” in the same sense as normal distributions [103]. After all, a forward proton must survive very different final-state interactions in, say, proton-antiproton scattering than in DIS. There are growing data on single, and double diffraction in hadron-hadron scattering with which to compare [104, 105]. Data on the detailed distributions of the forward proton in DIS are becoming accessible using the forward proton and neutron spectrometers at ZEUS [106] and H1 [107, 108].

Some of the most striking data on diffraction are with exclusive final states, $X = \omega, \rho, \psi$, etc. In this case, the perturbative scattering is required to be color singlet in both amplitude and complex conjugate. This requires a minimum of *two* partons for each, so that the exclusive diffraction amplitude begins at twist four, scaling as $1/M_X^2 \sim 1/[(1-x_{\mathcal{P}})Q^2]$. When M_X is large and t is small the amplitude for this process is described by the same sort of asymmetric distribution probed in DVCS above [109, 110]. If we assume that the hard scattering is initiated by the exchange of two gluons, it is natural to identify this amplitude with the gluon density, $G(x_{\mathcal{P}}, M_X) \sim x^{-\lambda(M_X)}$, where we approximate the steep increase of $G(x, M_X)$ at small $x = x_{\mathcal{P}}$ and moderate M_X by a power, increasing with M_X (see Fig. 5). Since $W^2 \sim 1/x$, the cross section, which is proportional to the square of this amplitude, behaves as

$$\frac{d\sigma^D}{dM_X} \sim \frac{1}{M_X^4} W^{4\lambda(M_X)}. \quad (33)$$

There is now considerable evidence in diffractive vector boson production supporting this general picture [18]. The example of Fig. 12 shows the steepening of the W -dependence of ρ - and ϕ -production for various values of Q^2 .

The phenomenology of diffraction has inspired a number of well-motivated physical models, which should be thought of as shedding complementary light on this set of processes. Each was extensively discussed at the workshop.

In the model of Ingelman and Schlein [111], hard diffraction probes the partonic structure of the pomeron,

$$f_{a/\mathcal{P}}^D = f_{a/\mathcal{P}} \otimes f_{\mathcal{P}/p}, \quad (34)$$

where $f_{a/\mathcal{P}}(\beta)$ is the distribution of parton a in the pomeron, while $f_{\mathcal{P}/p}$ is the distribution of pomerons in the proton. There is as yet no field-theoretic justification

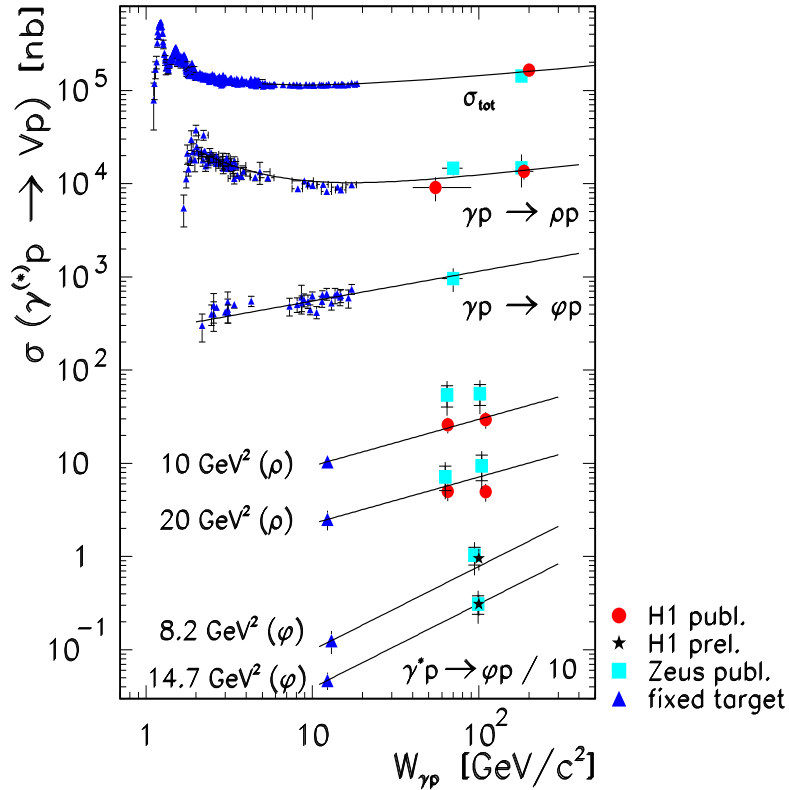


Figure 12: ρ and ϕ production cross section as a function of W for several values of Q^2 [7].

of this picture, which differs from Eq. (32) above in assuming an extra convolution. Still, it has provided a valuable starting-point for the analysis of triply-differential structure functions [103]. These generally require a very hard gluon distribution in the pomeron, $f_{g/p}(\beta)$, peaked near $\beta \sim 1$. An example of the evidence for this conclusion is shown in Fig. 13, in which the average $\int dx F_2^{D(3)}$ is plotted as a function of Q^2 [100]. Fits with a very hard gluon distribution account for the rise with momentum transfer. In addition, for $x_{\mathcal{P}} < 1$, fits based on a pomeron alone seem not to be able to account for the data, suggesting the need for an additional coherent object, generically a “reggeon”, \mathcal{R} , whose partonic structure is probed in the same fashion, but whose distribution $f_{\mathcal{R}/p}$ is less singular as $x_{\mathcal{P}} \rightarrow 1$ [7].

In the color dipole model [112, 113, 114, 115], the photon couples to a quark pair, which interacts with the proton by the exchange of two gluons. Here the twist, and therefore Q -dependence of the process depends on the polarizations of these exchanges. When both gluons carry physical polarizations, the process is higher-twist, but includes a color-singlet component, and can describe exclusive vector boson production, as above. When one of the gluons carries an unphysical polarization, the process can be leading twist, and is suitable for describing inclusive diffraction. The interplay of polarization and color exchange is particularly well illustrated in recent

H1 Preliminary 1994

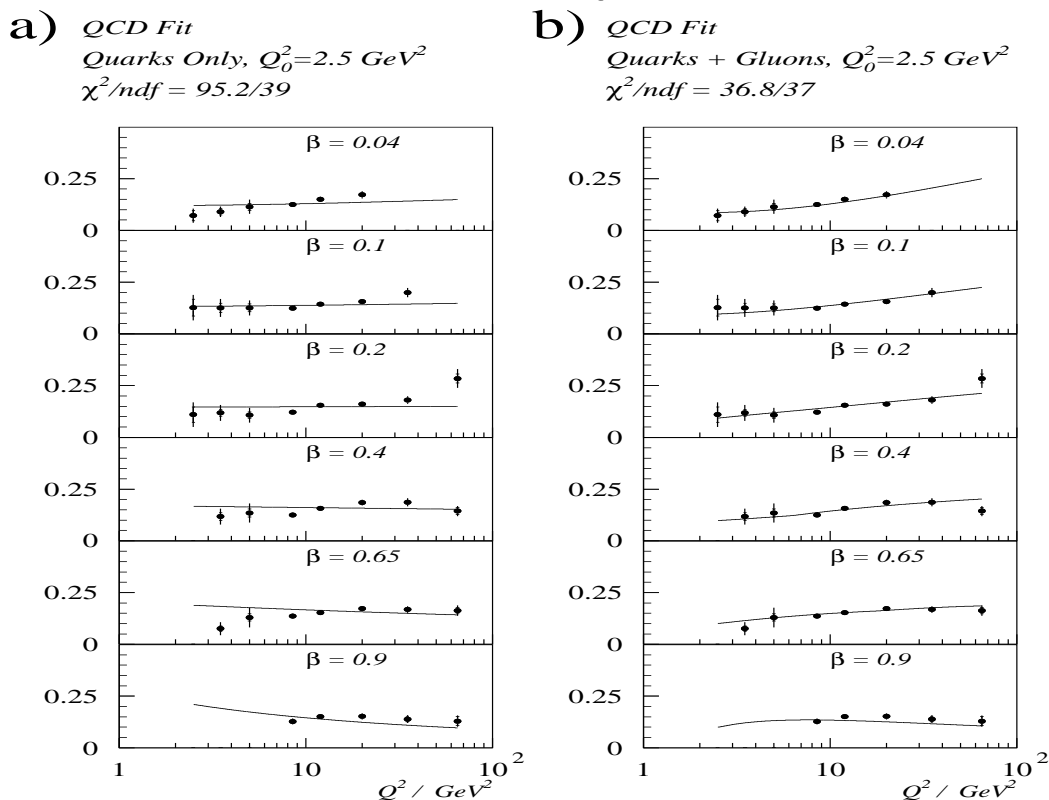


Figure 13: QCD fit for the average of $F_2^{(D)}$ (a) with quarks only, (b) with hard gluon component [100].

work described at the workshop on “semiclassical” models, in which, as in the dipole model, the pair is pictured as interacting with a background classical color field while passing through the target proton [116, 117, 118]. The simplification of the coupling of the semiclassical background field to the color dipole bears a close relation to the factorization of soft gluons from jets in perturbative proofs of factorization theorems [119].

One of the virtues of the color dipole model is that it allows the investigation of higher- and leading-twist effects within a single framework. Such an analysis [114] suggests that as $\beta \rightarrow 1$, higher twist may dominate for a wide range of Q . If so, the apparent peak near $\beta = 1$ of $f_{g/P}(\beta)$, referred to above, may be the result of a restriction to a leading twist fit.

4.4 Rapidity Gaps in Jet Production at the Tevatron

The interplay between short- and long-distance interactions is well-illustrated by the rapidity gaps in jet production observed at the Tevatron. Unlike the diffractive events discussed above, partons from both the beams appear to undergo hard scatterings, producing pairs of jets. In a detectable fraction of events, however, there is little or no

radiation in the rapidity range between the jets [120, 121]. This is normally attributed to the exchange of strongly interacting partons in a color singlet configuration, a “hard pomeron”, which complements the high- Q^2 diffractive vector boson production discussed above. These events are more difficult to study, however, because their large momentum transfers make them rare, and because they are masked by unconnected “spectator-spectator” interactions which reduce their “survival” in the final state. We may hope, however, for progress in the theory of rapidity gap events, as more is learned about the role of color exchange in hard cross sections [122].

5 Power Corrections: Openings to Nonperturbative Physics

As we have noted above, perturbative QCD predictions at NLO are most accurate when the cross section is sensitive to only a single large scale. Jet cross sections and event shapes, although IR safe, remain sensitive to hadronization scales even at quite high energies, as at LEP [123]. Event generators have been remarkably successful in modeling such cross sections, but they are bound to mask some of the physics in adjustable parameters.

One of the important developments of the past year has been a new willingness to step back from event generators and to confront perturbative computations directly to the data. In jet cross sections, the discrepancy between NLO (or NNLO) theory and experiment is rather large, of the order of tens of percent, but shows a characteristic power decay, as $1/Q$ or $1/Q^2$, depending on the quantity tested. DIS experiments are ideal for the study of such effects, since Q can be varied in a single experiment.

The impetus for this reanalysis has come from theory [124, 125, 126, 127, 128, 129]. The basic observation is that when we calculate an IR safe cross section, we do not eliminate contributions from soft partons altogether. Rather, they typically occur in integrals of the generic form,

$$\frac{1}{Q^a} \int_0^Q d^{a+2b}k \frac{1}{(k^2)^b}. \quad (35)$$

with $a > 0$, where k denotes some set of loop momenta. Any integral of this sort is infrared finite, and the region of soft loop momenta, $k < Q_0$, with Q_0 fixed, contributes a “power correction”, $(Q_0/Q)^a$. Normally, such corrections are simply absorbed into the IR safe coefficients of the strong coupling. On the other hand, we really do not know how soft gluons contribute, and we certainly expect that for $Q_0 \sim \Lambda_{\text{QCD}}$, nonperturbative scales will become important.

For many IRS quantities, it is possible to reorganize (resum) perturbation theory into a form in which the running coupling itself signals the introduction of nonperturbative scales. Consider, for example, the thrust T_C , defined in DIS as

$$T_C = \max_{\hat{n}} \frac{\sum_i |p_i \cdot \hat{n}|}{\sum_i |p_i|}, \quad (36)$$

where the sum is over all hadrons in the Breit-frame hemisphere of the scattered quark, and the maximum is over unit directions. T_C , which is frame dependent, is maximized to unity when all the hadrons line up in a single jet. At lowest order in perturbation theory, the final state is a quark pair, and $T_C = 1$ exactly. We thus naturally consider $1 - T_C$,

$$1 - T_C = \frac{1}{Q} \sum_i (|p_i| - |p_i \cdot \hat{n}|). \quad (37)$$

The contribution to $1 - T_C$ of a single soft gluon emitted by the quark is given approximately by

$$\Delta_{1-T_C}^{(1)} = \int \frac{dk_T^2}{k_T^2} C_F \frac{\alpha_s(k_T)}{\pi} \int_{k_T}^Q \frac{dk_0}{\sqrt{k_0^2 - k_T^2}} \frac{k_0 - \sqrt{k_0^2 - k_T^2}}{Q}. \quad (38)$$

Here we have let the coupling run with k_T , the momentum component transverse to the quark axis, so that the probability to emit the extra gluon grows when the gluon becomes either soft, or collinear to the quark. The k_0 integral may be carried out explicitly, and leads to an integral of the form of Eq. (35) above,

$$\Delta_{1-T_C}^{(1)} = \frac{1}{Q} \frac{C_F}{\pi} \int_0^Q dk_T \alpha_s(k_T). \quad (39)$$

For k_T large enough, the integrand makes perfect sense, but when k_T is soft, we are led to modify the perturbative expression to make it finite, and introduce a new, nonperturbative parameter with units of mass, which controls the $1/Q$ correction to the thrust distribution. We have seen at this workshop how expressions derived in this way can model thrust and other event shape distributions at HERA surprisingly well, in terms of only a few new parameters of this kind. Examples are shown in Fig. 14 [130].

Similar analyses have been carried out for e^+e^- annihilation, but the variable hard scattering scale Q^2 in DIS makes it ideal for studying effects of this kind. These effects are closely related to nonperturbative contributions to k_T broadening in Z and Drell-Yan pair production in hadron-hadron scattering [10], and undoubtedly to the single-photon spectra discussed above [64]. I believe there is a strong chance that a unified picture of such effects, cutting across a variety of processes, will lead to important new insights in the coming year or two.

Unfortunately, there is no space here to discuss other theoretical investigations of nonperturbative effects in high energy processes, including new studies of shadowing, of the roles of instantons in DIS, and reports of progress in the lattice computation of parton distributions. As these presentations demonstrated, however, QCD remains a fascinating subject of inquiry at all length scales.

6 Where are we now?

What is the place of DIS, the significance of QCD studies? Whether or not the HERA high- Q^2 events turn out to be a discovery of historic proportions or a trick

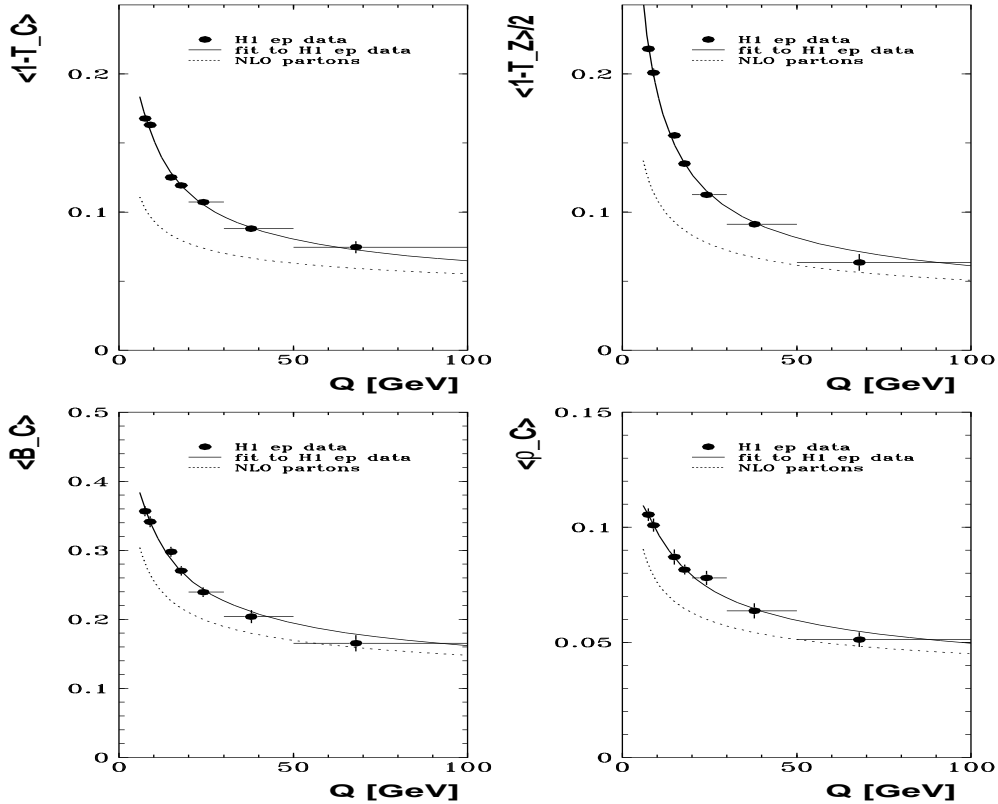


Figure 14: Event shapes plotted against Q , and compared to NLO calculations and fits including $1/Q$ corrections [130].

of statistics, they highlight the potential of deeply inelastic scattering for discovery, and the importance of an improved “standard model” of quantum chromodynamics. This is certainly a viewpoint that finds a wide resonance in the physics community. There is another viewpoint, represented at the workshop, although not always stated explicitly. This is that the study of quantum chromodynamics and the investigation of hadronic scattering are the most challenging problems in quantum field theory that are currently accessible in the laboratory. This tradition predates QCD, and was first posed in the context of a very different theoretical context. It was deeply inelastic scattering that brought on a new age – the age of the parton, then of QCD, which changed the set of questions that most theorists wanted to ask.

It is once again DIS, in a series of advances at HERA, monitored by the four preceding DIS conferences, which has led us back to some of the old questions, which we are finally ready to address again, in the new context of quantum field theory. First the small- x data on structure functions, then the surprising frequency of diffractive events, the wealth of photoproduction data, all bring us to the interface of nonperturbative and perturbative physics, which truly distinguishes QCD as “the” field theory of the standard model. At this interface, our knowledge is very uneven, progress is halting, and models have an important role to play. At the same time, perturbative

methods have been found to be surprisingly, sometimes amazingly, flexible, when the right questions are asked. We must use the QCD we know well to investigate new physics; but we must also pursue the QCD we do not know well.

Acknowledgments

I would like to thank the Organizing Committee, and especially José Repond, for inviting me, and for invaluable help during the workshop and in the preparation of the manuscript. I would also like to thank the Session Convenors of DIS 97 for sharing many insights, and Vittorio Del Duca, Fred Olness, Anatoly Radyushkin and Marek Zielinski for very helpful conversations. This work was supported in part by the National Science Foundation under grant PHY 9309888.

References

- [1] E. Kabuss, Working Group I, these Proceedings.
- [2] R. Bernstein, Working Group I, these Proceedings.
- [3] A. Magnon, Working Group IV, these Proceedings.
- [4] Z. Meziani, Working Group IV, these Proceedings.
- [5] R.G. Roberts, Plenary Session, these Proceedings.
- [6] R. Nania, Plenary Session, these Proceedings.
- [7] G. Bernardi, Plenary Session, these Proceedings.
- [8] T. Carli, Working Group I, these Proceedings.
- [9] F. Zarnecki, Working Group I, these Proceedings.
- [10] H.E. Montgomery, Plenary Session, these Proceedings.
- [11] J. Forshaw, Plenary Session, these Proceedings.
- [12] Yu.L. Dokshitzer, Plenary Session, these Proceedings.
- [13] R. Milner, Plenary Session, these Proceedings.
- [14] R. Yoshida and J. Blümlein, reports of Structure Function Working Group (I), this Proceedings.
- [15] A. Doyle, report of Hadron Final State Working Group (III), this Proceedings.
- [16] E. Levin and S. Forte, reports of Theory Working Group (V), these Proceedings.
- [17] T. Gehrmann, report of Spin Working Group (IV), these Proceedings.

- [18] D. Soper and P. Newman, reports of Diffraction Working Group (II), this Proceedings.
- [19] ZEUS Collaboration, hep-ex/9702015.
- [20] H1 Collaboration, hep-ex/9702012.
- [21] D. Zeppenfeld, Working Group I, these Proceedings.
- [22] J. Blümlein, Working Group I, these Proceedings.
- [23] S. Lola, Working Group I, these Proceedings.
- [24] G. Wang, Working Group I, these Proceedings.
- [25] X. Tata, in *QCD and Beyond*, Proceedings of the Theoretical Advanced Study Institute in Elementary Particle Physics, 1995, Ed. D. Soper, Singapore, World Scientific, 1996, p. 163.
- [26] G. Altarelli *et al.*, hep-ph/9703276.
- [27] J. Kalinowski, Working Group I, these Proceedings.
- [28] C.S. Wood *et al.*, *Science* **275**, 1759 (1997).
- [29] S. Kuhlmann, Working Group I, these Proceedings.
- [30] A. White, Working Group I, these Proceedings.
- [31] G. Altarelli and G. Parisi, *Nucl. Phys.* **B126**, 298 (1977);
V.N. Gribov and L.N. Lipatov, *Sov. J. Nucl. Phys.* **15**, 438, 675 (1972);
Yu.L. Dokshitzer, *Sov. Phys. JETP* **46**, 641 (1977).
- [32] P. Spentzouris, Working Group I, these Proceedings.
- [33] M. Schmelling, *28th International Conference on High Energy Physics*, Warsaw, 1996, Z. Ajduk and A.K. Zroblewski Editors, Singapore, World Scientific, 1997.
- [34] A. Meyer, Working Group I, these Proceedings.
- [35] B. Surrow, Working Group I, these Proceedings.
- [36] M.A.J. Botje, Working Group I, these Proceedings.
- [37] J. Roldan, Working Group I, these Proceedings.
- [38] F. Zomer, Working Group I, these Proceedings.
- [39] A. Wegner, Working Group III, these Proceedings.
- [40] M. Glück, E. Reya and A. Vogt, *Z. Phys.* **C67**, 433 (1995).

- [41] D. Haidt, Working Group I, these Proceedings.
- [42] B. Badelek, Working Group I, these Proceedings.
- [43] A. Donnachie and P.V. Landshoff, *Z. Phys.* **C61**, 139 (1994).
- [44] J. Kwieciński, A.D. Martin and A.M. Stasto, Working Group I, these Proceedings.
- [45] É.A. Kuraev, L.N. Lipatov, V.S. Fadin, *Sov. Phys. JETP* **45**, 199 (1977);
Ya.Ya. Balitskii and L.N. Lipatov, *Sov. J. Nucl. Phys.* **28**, 822 (1978).
- [46] A. Kovner, Working Group V, these Proceedings.
- [47] R. Ball, Working Group V, these Proceedings.
- [48] A.H. Mueller and H. Navelet, *Nucl. Phys.* **B282**, 727 (1987).
- [49] C.R. Schmidt, *Phys. Rev. Lett.* **78**, 4531 (1997).
- [50] S.Y. Jun, Working Group III, these Proceedings.
- [51] S. Wölflé, Working Group III, these Proceedings.
- [52] D. Zeppenfeld, Working Group III, these Proceedings.
- [53] V. Fadin, Working Group V, these Proceedings.
- [54] V. Del Duca, Working Group V, these Proceedings.
- [55] R.S. Thorne, Working Group I, these Proceedings.
- [56] E. Laenen and G. Sterman, in preparation.
- [57] G. Sterman, *Nucl. Phys.* **B281**, 310 (1987); S. Catani and L. Trentadue, *Nucl. Phys.* **B327**, 323 (1989); *Nucl. Phys.* **B353**, 183 (1991).
- [58] F. Zomer, Working Group III, these Proceedings.
- [59] D. Mikunas, Working Group III, these Proceedings.
- [60] J. Huston, Working Group III, these Proceedings.
- [61] D.A. Kosower, Working Group I, these Proceedings.
- [62] A.D. Martin, R.G. Roberts and W.J. Stirling, *Phys. Rev.* **D50**, 6734 (1994).
- [63] H.L. Lai *et al.*, *Phys. Rev.* **D51**, 4763 (1995).
- [64] M. Zielinski, Working Group I, these Proceedings.
- [65] R. Blair, Working Group I, these Proceedings.

- [66] R. Saunders, Working Group III, these Proceedings.
- [67] T. Ebert, Working Group III, these Proceedings.
- [68] J. Lamoureux, Working Group III, these Proceedings.
- [69] W.K. Tung, Working Group V, these Proceedings.
- [70] R.G. Roberts, Working Group V, these Proceedings.
- [71] H.L. Lai, Working Group I, these Proceedings.
- [72] F. Olness, Working Group I, these Proceedings.
- [73] R. Hirosky, Working Group III, these Proceedings.
- [74] T. Joffe-Minor, Working Group III, these Proceedings.
- [75] M. Beneke, I.Z. Rothstein and M. Wise, hep-ph/9703429.
- [76] R.K. Ellis, W.J. Stirling and B.R. Webber, *Collider Physics*, Cambridge, Cambridge University Press, 1996.
- [77] W. Kilgore, Working Group III, these Proceedings.
- [78] A. Signer and L. Dixon, *Phys. Rev. Lett.* **78**, 811 (1997); and hep-ph/9706285.
- [79] T. van Ritbergen, Working Group I, these Proceedings.
- [80] D.A. Kosower, Working Group V, these Proceedings.
- [81] Z. Bern, Working Group V, these Proceedings.
- [82] L. Magnea, Working Group V, these Proceedings.
- [83] J. Blümlein, Working Group IV, these Proceedings.
- [84] D. Robaschik, Working Group IV, these Proceedings.
- [85] M. Stratmann, Working Group IV, these Proceedings.
- [86] P. Zyla, Working Group IV, these Proceedings.
- [87] G. Ridolfi, Working Group IV, these Proceedings.
- [88] T. Gehrmann, Working Group IV, these Proceedings.
- [89] C. Coriano, Working Group IV, these Proceedings.
- [90] B. Ermolaev, Working Group IV, these Proceedings.
- [91] U. Stösslein, Working Group IV, these Proceedings.

- [92] A. De Roeck, Working Group IV, these Proceedings.
- [93] A. Magnon, Working Group IV, these Proceedings.
- [94] E. Kabuss, Working Group IV, these Proceedings.
- [95] P. Schüler, Working Group IV, these Proceedings.
- [96] A.V. Radyushkin, Working Group IV, these Proceedings.
- [97] P. Guichon, Working Group IV, these Proceedings.
- [98] X. Ji, *Phys. Rev.* **D55**, 7114 (1997).
- [99] M. Grothe, Working Group II, these Proceedings.
- [100] M. Dirkmann, Working Group II, these Proceedings.
- [101] D. Soper, Working Group II, these Proceedings.
- [102] A. Berera, Working Group II, these Proceedings.
- [103] J. Whitmore, Working Group II, these Proceedings.
- [104] P. Melese, Working Group II, these Proceedings .
- [105] A. Brandt, Working Group II, these Proceedings.
- [106] N. Cartiglia, Working Group II, these Proceedings.
- [107] B. List, Working Group II, these Proceedings.
- [108] D. Jansen, Working Group II, these Proceedings.
- [109] A.V. Radyushkin, Working Group II, these Proceedings.
- [110] A. Freund, Working Group II, these Proceedings.
- [111] G. Ingleman and P.E. Schlein, *Phys. Lett.* **B152**, 256 (1985).
- [112] N.N. Nikolaev, Working Group II, these Proceedings.
- [113] M. Wüsthoff, Working Group II, these Proceedings.
- [114] J. Bartels, Working Group II, these Proceedings.
- [115] C. Royon, Working Group II, these Proceedings.
- [116] M. McDermott, Working Group II, these Proceedings.
- [117] A. Hebecker, Working Group II, these Proceedings.
- [118] W. Buchmuller, Working Group II, these Proceedings.

- [119] J.C. Collins, D.E. Soper and G. Sterman, in *Perturbative Quantum Chromodynamics*, A.H. Mueller Editor, Singapore, World Scientific, 1989, p. 1.
- [120] J. Perkins, Working Group II, these Proceedings.
- [121] A. Bhatti, Working Group II, these Proceedings.
- [122] N. Kidonakis, Working Group V, these Proceedings.
- [123] DELPHI Collaboration (P. Abreu *et al.*), *Z. Phys.* **C73**, 229 (1997).
- [124] M. Beneke, Working Group V, these Proceedings.
- [125] M. DasGupta, Working Group III, these Proceedings.
- [126] R. Akhoury, Working Group V, these Proceedings.
- [127] G. Marchesini, Working Group V, these Proceedings.
- [128] G. Sterman, Working Group V, these Proceedings.
- [129] M. Sotiropoulos, Working Group V, these Proceedings.
- [130] K. Rabbertz, Working Group III, this Proceedings.